Genomic and phenotypic comparisons reveal distinct variants of *Wolbachia* strain *w*AlbB

Julien Martinez[a#], Perran A. Ross[b], Xinyue Gu[b], Thomas H. Ant[a], Shivan M. Murdochy[a], Lily Tong[a], Ana da Silva Filipe[a], Ary A. Hoffmann[b], Steven P. Sinkins[a#]

[a]MRC-University of Glasgow Centre for Virus Research, Glasgow, UK

[b]Pest and Environmental Adaptation Research Group, Bio21 Institute, the University of Melbourne, Parkville, VIC, Australia

[#] Address correspondence to Julien Martinez, julien.martinez@glasgow.ac.uk. Co-corresponding author: Steven P. Sinkins, steven.sinkins@glasgow.ac.uk.

J.M. and P.A.R. contributed equally to this work. Author order was determined based on higher relative contribution of J.M. to experimental planning.

Running title: Characterization of *Wolbachia* strain *w*AlbB variants

Abstract word count: 198

Main text word count: 5,805

Abstract

The intracellular bacterium *Wolbachia* inhibits virus replication and is being harnessed around the world to fight mosquito-borne diseases through releases of mosquitoes carrying the symbiont. *Wolbachia* strains vary in their ability to invade mosquito populations and suppress viruses in part due to differences in their density within the insect and associated fitness costs. Using whole-genome sequencing, we demonstrate the existence of two variants in *w*AlbB, a *Wolbachia* strain being released in natural populations of *Aedes aegypti* mosquitoes. The two variants display striking differences in genome architecture and gene content. Differences in the presence/absence of 49 genes between variants include genes located in prophage regions and others potentially involved in controlling the symbiont's density. Importantly, we show that these genetic differences correlate with variation in *w*AlbB density and its tolerance to heat stress, suggesting that different *w*AlbB variants may be better suited for field deployment depending on local environmental conditions. Finally, we found that the *w*AlbB genome remained stable following its introduction in a Malaysian mosquito population. Our results highlight the need for further genomic and phenotypic characterization of *Wolbachia* strains in order to inform ongoing *Wolbachia*-based programmes and improve the selection of optimal strains in future field interventions.

Importance

Dengue is a viral disease transmitted by *Aedes* mosquitoes that threatens around half of the world population. Recent advances in dengue control involve the introduction of *Wolbachia* bacterial symbionts with antiviral properties into mosquito populations which can lead to dramatic decreases in the incidence of the disease. In light of these

promising results, there is a crucial need to better understand the factors affecting the success of such strategies, in particular the choice of *Wolbachia* strain for field releases and the potential for evolutionary changes. Here we characterized two variants of a *Wolbachia* strain used for dengue control that differ at the genomic level and in their ability to replicate within the mosquito. We also found no evidence for the evolution of the symbiont within the two years following its deployment in Malaysia. Our results have implications for current and future *Wolbachia*-based health interventions.

Introduction

Aedes aegypti mosquitoes are the primary vectors of dengue, a neglected viral disease ranked by WHO among the top ten global health threats, with 50–100 million clinically apparent cases and half a million hospitalizations for severe disease every year (1). Current control methods based on insecticide fogging for mosquito suppression have failed to halt the continued expansion in range and incidence of dengue, and rising levels of insecticide resistance mean that there is a pressing need for innovative approaches. *Wolbachia* are maternally inherited symbiotic bacteria found in many insect species, but not naturally in *Ae. aegypti* (Ross et al. 2020); however following lab transfer into this species some *Wolbachia* strains can efficiently block dengue transmission (3–6), by causing perturbations in various cellular pathways including lipid transport (7).

Wolbachia strains *w*Mel from *Drosophila melanogaster* and *w*AlbB from *Aedes albopictus* have both been shown to spread to and remain at a high frequency in *Ae. aegypti* populations following releases of *Ae. aegypti* at a comparatively modest scale and

duration without needing continuous re-introduction (8–11). These strains have a self-spreading capability using a form of reproductive manipulation known as cytoplasmic incompatibility (CI), whereby the progeny of *Wolbachia*-carrying males and *Wolbachia*-free females die, while the reverse cross is fertile, giving an advantage to *Wolbachia*-carrying females. Both strains have been shown to efficiently reduce dengue transmission, providing a safe, sustainable, cost-effective and eco-friendly biocontrol tool that holds great promise for reducing the global burden of dengue (8, 11–14).

Since releases of *Ae. aegypti* carrying *w*AlbB (6) were carried out in Malaysia in sites around Kuala Lumpur that were previously hot-spots for dengue transmission, dengue has been substantially decreased (8). When larvae develop under high temperature regimes with diurnal peaks around 37°C, *w*AlbB is more stable than *w*Mel, maintaining a higher density, high maternal transmission and efficient dengue transmission blocking (6, 15–18). The fitness cost of *w*AlbB in *Ae. aegypti* is higher than *w*Mel in lab assays, mainly due to slightly reduced adult longevity (6) and reduced fertility and fecundity of adult females produced from quiescent eggs (19). *Wolbachia* fitness costs negatively affect population dynamics, raising the threshold frequency that must be exceeded for CI-mediated spread to occur (20–22) and for *Wolbachia* to remain at stable high frequency after introduction, as occurred with *w*AlbB at a number of sites in Malaysia (8). Several independent transinfections of *w*AlbB from *Ae. albopictus* have been generated in *Ae. aegypti* through microinjection (6, 23, 24) and two of these have been released in natural populations (8, 25). While the transinfections originate from different geographic locations, it is unclear if there are genetic or phenotypic differences between them.

The effectiveness of *Wolbachia* interventions against dengue could be compromised in the longer term by evolutionary changes in the *Wolbachia* or mosquito genome (26). Virus transmission blocking could be reduced over time if mosquito-*Wolbachia* co-evolution results in lower *Wolbachia* density overall, or more restricted tissue distribution to the ovaries and testes. The *w*AlbB-associated reduced hatch rate of stored *Ae. aegypti* eggs could also be ameliorated by natural selection (27); if this selection acts specifically at the egg stage and does not impact the dengue transmission-blocking phenotype, it would be advantageous overall for implementation of the strategy. No obvious phenotypic changes have been observed in *w*AlbB to date in field populations of *Ae. aegypti* (18) but longer-term monitoring is required.

The primary aim of this study was to sequence the genome of the *w*AlbB strain released in Malaysia. This is useful for several reasons: to be able to ascertain whether this *w*AlbB has any unique genomic features relative to previously published *w*AlbB genomes; to be able to track genomic evolution that may occur in the field, that could potentially compromise the effectiveness of the dengue intervention; and to allow for the creation of molecular assays to allow this variant to be distinguished from the naturally occurring *w*AlbB present in *Ae. albopictus*, which will be useful in *Wolbachia* frequency monitoring, since both species are present in the intervention sites. Other aims were to compare the impact of different *w*AlbB infections on *Wolbachia* density, egg quiescence and responses to heat.

Results

Comparative genomics of *w*AlbB genomes

We compared three publicly available *w*AlbB circular genomes (Texas, Florida and Hainan) with a new draft assembly that we generated from an Indonesian *w*AlbB infection previously transferred into *Ae. aegypti* (6) (Figure 1A). The Indonesian *w*AlbB assembly was 1.45 Mb in size, >99% of which was made of 9 contigs (Table 1). This is slightly shorter than finished *w*AlbB genomes (1.48 Mb), however, similar numbers of single-copy conserved orthologues were found between *w*AlbB genomes suggesting the *w*AlbB-II assembly is nearly complete (Table 1). In light of the genomic differences described below, we will refer to *w*AlbB-I and *w*AlbB-II to designate the reference variant from Texas and the Indonesian variant respectively.

The Indonesian *w*AlbB-II variant clusters with the three other available *w*AlbB genomes into a monophyletic clade within *Wolbachia* supergroup B (Figure 1B). However, despite the strong phylogenetic relatedness, *w*AlbB-II displays striking differences in genome synteny when compared to *w*AlbB-I and the *w*AlbB-I-like genomes originating from Florida and China (Figure 1A). There are three incomplete WO prophage regions in the *w*AlbB-II genome, indicating ancient WO phage infections. The structural and non-structural modules (head, tail, baseplate, replication and eukaryotic modules) are split between the different regions, suggesting no active phage replication (Figure 2). Moreover, essential genes of the phage head, tail and baseplate are missing indicating that the production of phage particles is impaired (Table 2). Core phage genes are present in single copies except for the recombinase and phospholipase D which are both present in two copies with high sequence divergence, suggesting that the *w*AlbB genome may have been

colonized in the past by more than one WO phage (Table 2). The other *w*AlbB genomes also carry prophage regions with sequence similarities to those of *w*AlbB-II but these have rearranged into five different regions (Figure 1A). Two pairs of the cytoplasmic incompatibility-inducing genes *cifA* and *cifB* are located within *w*AlbB-II's prophage regions and are identical to the other *w*AlbB genomes. The two gene pairs are related to type III *cif* homologues for one pair and type IV for the other pair as defined in previous studies (28, 29).

In addition to chromosomal rearrangements, we found noticeable differences in gene content between the *w*AlbB-I-like and *w*AlbB-II genomes (Figure 1C, Table S1), with ~70% of the differences involving repeat elements (transposases, group II introns reverse-transcriptase and related pseudogenes). Excluding repeat elements, *w*AlbB-II harbours 23 genes that are absent from or pseudogenized in the three other genomes, while on the other hand, *w*AlbB-I, -FL2016 and -HN2016 share 26 genes not found or pseudogenized in the *w*AlbB-II draft assembly. Some of this variation is located within and around prophage regions, where *w*AlbB-II and the other *w*AlbB genomes have lost different core and accessory phage genes (Figure 2, Table 2, Table S1). For instance, one of the *w*AlbB-II phage eukaryotic modules lacks two copies of a putative transcriptional regulator and one copy of a DNA repair protein which are homologues of genes in an eight-gene locus know as Octomom thought to influence *Wolbachia* proliferation in *w*Mel-like strains (30–32) (Figure 2A). Interestingly, *w*AlbB-II also carries two syntenic proteins (WP_019236968.1 and WP_019236969.1) with homologies to arthropod protein translocase subunit secA genes that are absent in other *w*AlbB genomes (Table S1) but present in other *Wolbachia* strains. The two genes are of unusual length for *Wolbachia*

156 genes. They branch with a few other *Wolbachia* homologues within arthropod lineages
157 with no closely-related bacterial homologues indicating two independent horizontal
158 transfers from arthropods to *Wolbachia* in the case of WP_019236968.1 and at least one
159 such event for WP_019236969.1 (Figures S2). Finally, several genes differed between
160 *w*AlbB variants due to pseudogenization by the insertion of a transposon. For example, a
161 homologue of the *Wolbachia* surface protein *wspB*, is pseudogenized in the three *w*AlbB-
162 I-like genomes while a full-length version of the gene is present in *w*AlbB-II.

163 It is possible that some of the genes predicted to be absent in *w*AlbB-II might in fact be
164 present but were not assembled. For instance, one of *w*AlbB-II contigs showed a 2x
165 sequencing depth compared with the rest of the assembly and is identical to a large region
166 that is duplicated in the other *w*AlbB genomes (asterisks in Figure 1A, Table S1). Similarly,
167 another three-gene duplication in *w*AlbB-I genomes also displayed a 2x sequencing depth
168 in *w*AlbB-II (Table S1). Thus, we counted the extra copies of genes in these two large
169 duplications as present in *w*AlbB-II. Nevertheless, we confirmed that all other genes
170 missing in *w*AlbB-II (excluding transposable elements) were either present but annotated
171 as pseudogenes or that no *w*AlbB-II Illumina reads mapped to the corresponding genes
172 in the other genomes (Table S1, Figure S1).

173 Numerous single nucleotide polymorphisms (SNPs) and small indels between the *w*AlbB
174 genomes were identified (Table 3, Table S2). In reciprocal comparisons, there were more
175 polymorphisms when *w*AlbB-II was used as the reference genome for SNP calling. This
176 is likely because the *w*AlbB-II assembly is incomplete, which may generate false-positives
177 within misassembled repeat sequences. This is supported by the fact that five SNPs were
178 detected in transposable elements when mapping *w*AlbB-II reads on its own assembly.

Moreover, the five SNPs were all polymorphic upon visual inspection of the mapped reads. Nevertheless, *w*AlbB-II showed the smallest number of SNPs against *w*AlbB-I, while it was more divergent from *w*AlbB-FL2016 and *w*AlbB-HN2016. This is inconsistent with the pattern of gene presence/absence observed above. However, a large proportion of SNPs against *w*AlbB-FL2016 and *w*AlbB-HN2016 displayed an atypical distribution with a few loci accumulating the majority of the SNPs. As noted in Ross et al. (2021), this could be due to possible DNA contamination in these two assemblies. Around 60% of the SNPs between *w*AlbB-II and *w*AlbB-I are non-synonymous, of which some are located within ankyrin repeat domain-containing genes as well as genes potentially involved in transcription and RNA processing (e.g. sigma factor RpoD (34), transcription elongation factor NusA (35), RNA polymerase subunit alpha and beta, ribonucleases E and D (36)), protein synthesis (e.g. ribosomal proteins, translational GTPase TypA (37)), cell wall synthesis and remodelling (e.g. N-acetylmuramoyl-L-alanine amidase, D-alanyl-D-alanine carboxypeptidase, M23 family peptidase, UDP-N-acetylmuramate dehydrogenase (38, 39)) and stress response (e.g. heat shock proteins: ATP-dependent Clp endopeptidase (40), DegQ endoprotease (41)).

***w*AlbB *Wolbachia* variants display background-dependent differences in density**

To determine potential effects of *w*AlbB variation on phenotype, we generated *Ae. aegypti* populations with different *Wolbachia* infection types (*w*AlbB-I, *w*AlbB-II or uninfected) and backgrounds (Australian (Au) or Malaysian (My)) through reciprocal backcrossing (33). *Wolbachia* density was influenced by *w*AlbB variant in both sexes (Table S3), with *w*AlbB-

I individuals having higher *Wolbachia* densities than *w*AlbB-II individuals (Figure 3A and B). We found no clear effect of nuclear background for either sex, but there was a significant interaction between nuclear background and *w*AlbB variant in males (Table S3). In the Australian background, *w*AlbB-I had a higher density than *w*AlbB-II (GLM: females: $F_{1,76} = 13.792$, $P < 0.001$, males: $F_{1,73} = 27.401$, $P < 0.001$) but there were no significant differences between variants in the Malaysian background (females: $F_{1,76} = 0.982$, $P = 0.325$, males: $F_{1,76} = 2.225$, $P = 0.140$).

To test the stability of *w*AlbB variants at high temperatures, we measured *Wolbachia* densities in adults after eggs were exposed to cyclical heat stress (29-39°C) or held at 26°C for one week. *Wolbachia* density was influenced by *w*AlbB variant and temperature treatment, with significant interactions between *w*AlbB variant and nuclear background as well as *Wolbachia* variant and temperature (Table S4). When the *w*AlbB-I and *w*AlbB-II variants were tested separately, we found no effect of temperature or nuclear background in either sex (all $P > 0.141$) for *w*AlbB-I, indicating that this infection is stable under heat stress (Figure 3C and D). In contrast, *w*AlbB-II density was lower in the heat stress treatment (Females: $F_{1,56} = 51.940$, $P < 0.001$, Males: $F_{1,56} = 61.814$, $P < 0.001$) and in the Malaysian background (Females: $F_{1,56} = 12.831$, $P = 0.001$, Males: $F_{1,56} = 4.549$, $P = 0.037$). Across both sexes and backgrounds, median *w*AlbB-II density under cyclical heat stress decreased by 80.4%, compared to 8.1% for *w*AlbB-I and 98.7% for *w*Mel.

Quiescent egg viability depends on mosquito nuclear background and *w*AlbB infection

Stored eggs from populations with different combinations of *w*AlbB infection type (*w*AlbB-I, *w*AlbB-II or uninfected), mitochondrial haplotype (Au or My) and background (Au or My) were hatched every three weeks to determine quiescent egg viability. *w*AlbB infection greatly reduced quiescent egg viability in all four combinations of background and mitochondrial haplotype (Figure 4). By week 16, hatch proportions for *w*AlbB-infected populations approached zero while hatch proportions for uninfected populations exceeded 40%. In uninfected populations, we found significant effects of egg storage duration and nuclear background on egg hatch proportions (Table S5). Eggs with an Australian background had higher hatch proportions (median 0.823) than eggs with a Malaysian background (median 0.503) by the end of the experiment. In *w*AlbB-infected populations, we found significant effects of egg storage duration, squared egg storage duration, nuclear background and replicate population (Table S5). Although populations carrying *w*AlbB-II had higher overall hatch proportions than *w*AlbB-I populations in both backgrounds (Figure 4), effects of *w*AlbB variant were not significant (Table S5). We had low power to detect *w*AlbB variant effects in this analysis due to nesting replicate population within *w*AlbB variant.

A multiplex PCR reaction for diagnostics of *w*AlbB variants

Given the genomic differences observed between the *w*AlbB genomes, we developed a PCR reaction allowing the distinction between the *w*AlbB-I and -II variants in *Ae. aegypti*

and *Ae. albopictus*. From our gene content analysis, we selected an AAA-family ATPase protein and the phage tail formation protein I as markers to distinguish the two *w*AlbB variants. Primers for these markers were designed and pooled with primers amplifying the 18S mosquito control gene into a multiplex PCR reaction. *w*AlbB-I in the Aa23 *albopictus* cell line and *w*AlbB-II in our *Ae. aegypti* mosquito lab line displayed the expected band profiles and were clearly distinguishable on the agarose gel (Figure 5). Moreover, the *w*AlbB infecting a Malaysian line of *Ae. albopictus* mosquitoes (JF) displayed identical bands to *w*AlbB-I variant.

No evidence for evolution of *w*AlbB-II genome following field release

Using the *w*AlbB-II assembly as a reference, we mapped the sequencing data generated from a *w*AlbB-infected *Ae. aegypti* colony *w*AlbB-MC (Mentari Court site) that was isolated from the field two years following field releases of wAlbB-II in Malaysia (18). All genome positions of the reference assembly were covered by read data from *w*AlbB-MC with no drastic drop in sequencing depth suggesting that no gene was lost since field releases (Figure S1A). Thirteen SNPs were detected, however, all were located within transposable elements (Table 3 and Table S2). Similar to *w*AlbB-II sequencing data, visual inspection of the *w*AlbB-MC mapped reads revealed that all SNPs were highly polymorphic indicating that they are likely false-positives caused by the use of an incomplete reference genome. Therefore, we conclude that there is little evidence for genomic changes that may have occurred following the introduction of *w*AlbB-II in the field.

Discussion

Here we uncovered major genomic differences between closely-related *w*AlbB-strain *Wolbachia* and showed these differences correlate with variation in symbiont density. *w*AlbB diversity has commonly been investigated using a limited number of markers such as the *wsp* gene and Multi-Locus Sequence Typing (MLST) genes with little to no variation observed between isolates from different locations (42–44). Whole-genome sequencing provides a higher resolution and has revealed significant genomic differences between closely-related *Wolbachia* strains (45–47). Using this method, we demonstrated the existence of at least two types of *w*AlbB variants that differ in genome synteny and gene content. The reference *w*AlbB-I variant originating from Texas and the *w*AlbB isolates from Florida and China share a similar genome architecture and gene content while the Indonesian *w*AlbB-II variant is strikingly different. Further sampling of *w*AlbB genomic diversity will provide new insights into the evolution of this symbiont lineage and may help unravel the colonization history of its native host, *Ae. albopictus*, across continents (48).

Importantly, there are differences in symbiont density between the *w*AlbB-I and *w*AlbB-II variants. Although only one isolate representative of each variant was characterised here, these results suggest that variant-specific genetic determinants may be driving some of the differences in density. It is possible, but less likely, that differences in mitochondrial haplotypes contributed to some of the variation in symbiont density since mitotypes were not cross-factored with the *w*AlbB variants. The reference isolates for *w*AlbB-I and II variants differed in the presence/absence of 49 genes (excluding transposable elements) and on ~200 SNPs, 60% of which were non-synonymous. How much of this variation contributes to differences in symbiont density remains to be investigated, and further

289 phenotypic characterisation of new variants will help shorten the list of candidate genes
290 since there is currently no transformation system in *Wolbachia* for functional validation.
291 Interestingly, some of the genomic differences are located within prophage regions. It has
292 been hypothesised that WO phage replication lowers *Wolbachia* density (49); however,
293 we only found incomplete prophage regions, suggesting that active phage mobilisation is
294 unlikely to occur in *w*AlbB. Alternatively, variation in the expression of phage accessory
295 genes could be responsible for differences in density. Indeed, *w*AlbB-I carries additional
296 copies of a DNA repair protein *radC* and a putative transcriptional regulator in its phage
297 eukaryotic module. Homologues of these genes in *w*Mel-like strains, WD0507 and
298 WD0508, are part of a 20 kb region called Octomom. Octomom is to date the only genetic
299 determinant shown to influence *Wolbachia* proliferation in a copy-number dependent
300 manner (30). Both complete loss of the region and amplification have been associated
301 with symbiont over-proliferation, which in turn has negative effects on host lifespan (31,
302 32).

303 Density variation could also stem from the way *w*AlbB variants interact with the host.
304 *Wolbachia* genomes commonly harbour an array of ankyrin domain-containing genes
305 which are predicted to be involved in protein-protein interactions as well as secretion
306 systems that may allow the export of bacterial effectors into the host cell cytoplasm (50,
307 51). Several ankyrin domain-containing genes are among the candidate genes that differ
308 between *w*AlbB variants. Additionally, *w*AlbB-II harbours two syntenic proteins showing
309 homologies to arthropod protein translocase subunit SecA genes. Homologues were
310 previously found in other *Wolbachia* strains (52) and their phylogenetic distribution points
311 towards an acquisition through horizontal transfer from a eukaryotic host. SecA proteins

312 are involved in the transport of bacterial and ER-exported proteins (53), suggesting that
313 the *w*AlbB variants may differ in the way they interact with the host cell. Interestingly,
314 *w*AlbB variants also differed in a homologue of the *Wolbachia* surface protein *wspB*. *wspB*
315 is pseudogenized in *w*AlbB-I and this variant maintains higher densities under a high
316 temperature cycle compared to *w*AlbB-II that carry a full-length version of the gene. This
317 is consistent with two recent studies showing that, among variants of the *Wolbachia* strain
318 *w*Mel, pseudogenization of the *wspB* gene is associated with variation in symbiont density
319 and maternal transmission and that the magnitude of this effect can vary with both
320 temperature and host background (54, 55). Finally, *w*AlbB variants differed in a number
321 of house-keeping genes involved in essential functions such as DNA replication, RNA
322 processing, translation or cell wall biogenesis that may contribute to the variation in
323 symbiont density, and in heat shock response genes that could potentially control their
324 different degrees of tolerance of heat stress.

325 The phenotypic differences detected impact on the relative ability of these variants to
326 spread through *Ae. aegypti* populations, and their efficacy for dengue control
327 programmes. The declining hatch rates over time of dried quiescent eggs is an important
328 component of the fitness costs of *w*AlbB in this host (19). In areas where a high proportion
329 of larval sites are temporary and experience intermittent inundation, dry eggs are often in
330 quiescence for extended periods, and thus the fitness cost of *w*AlbB will be higher relative
331 to *Wolbachia*-free wildtype counterparts than when larvae develop in permanent breeding
332 sites such as water storage tanks. This factor will increase the threshold population
333 frequency that must be exceeded for *Wolbachia* to spread / remain stable in the
334 population. The higher, background-dependent negative impact of the *w*AlbB-I on

quiescent egg hatch rates means that this variant will be predicted under some backgrounds / ecological conditions to spread less efficiently than *w*AlbB-II. Conversely the apparent slightly higher tolerance of *w*AlbB-I for very high temperature egg storage may also impact on relative spread dynamics, since maintenance of higher density of *w*AlbB-I may ultimately impact maternal transmission rates and virus inhibition. In the hottest climates in which *Ae. aegypti* occurs, *w*AlbB-I may prove to be a better option for dengue control than *w*AlbB-II. However, more data is needed under a variety of conditions and over multiple generations and life stages to test the relative impacts of temperature in more detail.

Previously, we found negligible changes in the *w*AlbB-I genome following transfer from its native host *Ae. albopictus* to *Ae. aegypti* (33) suggesting that there is little selective pressure to adapt to this new host, at least in laboratory conditions. This is in line with little genomic changes observed following artificial transfers of multiple *Wolbachia* strains between *Drosophila* species (56). Here we found no evidence of wAlbB-II genome evolution after its introduction in a field population of *Ae. aegypti*, which supports our earlier results showing stable density and antiviral effects using the same field-caught mosquito colony (18). It is also in line with the observed *w*Mel genome stability following the introduction of *Wolbachia*-infected *Ae. aegypti* mosquitoes in Australia (57, 58). *w*Mel and *w*MelPop-CLA infections in *Ae. aegypti* also show few long-term phenotypic changes following transinfection (10, 59).

Methods

Wolbachia purification

In order to generate Illumina sequencing data for both the reference *w*AlbB-II genome and its field-caught counterpart *w*AlbB-MC, *Wolbachia* was purified from whole mosquitoes. *w*AlbB-MC-infected mosquitoes were used after three generations spent in the lab since field collection in Mentari Court. For each genome, around 400 mosquitoes were collected into a 50 ml Falcon tube and snapped at -20°C for 10 min. Mosquitoes were then surface-sterilized for 3 min in 50% bleach, followed by 3 min in 70% ethanol and rinsed 3 times with sterile water. Mosquitoes were then manually homogenized with 3 mm glass beads in 40 ml of Schneider's media by shaking and further homogenized with a tissue-lyzer after transferring the homogenate into 2 ml tubes with 1 mm beads. Homogenates were centrifuged at 2,000 g for 2 min to remove tissue debris and the supernatant was sequentially filtered through 5, 2.7 and 1.5 µm sterile filters. The filtrate was aliquoted in Eppendorf tubes and centrifuged at 18,500 g for 15 min to pellet bacteria. The supernatant was discarded, Schneider's media added and the previous centrifugation step repeated once. The bacterial pellet was resuspended in Schneider's media and treated with DNase I at 37°C for 30 min to remove host DNA. Following digestion, samples were centrifuged at 18,500 g, the supernatant discarded and the DNase inactivated at 75°C for 10 min. Finally, bacterial pellets were pooled into one tube and DNA extracted with the Gentra Puregene tissue kit (Qiagen) with resuspension of the DNA pellet in 100 µl of nuclease-free water.

For long-read sequencing of the *w*AlbB-II genome, the same protocol was followed except that *Wolbachia* was purified from 150 freshly laid mosquito eggs. In order to increase the amount of starting DNA needed for Nanopore library construction, the DNA was amplified directly from the bacterial pellet before the DNA extraction step using the REPLI-G Midi kit (Qiagen).

Whole-genome sequencing and genome assembly

For both *w*AlbB-II and *w*AlbB-MC, DNA libraries were prepared using the Kapa LTP Library Preparation Kit (KAPA Biosystems, Roche7961880001) and sequenced on the Illumina MiSeq platform with the MiSeq Reagent Kit v3 to generate 2×150 bp reads. Raw reads were demultiplexed using bcl2fastq and adapters were trimmed with Trimmomatic v0.38.0 (60). To generate long reads for *w*AlbB-II, 1 µg of whole-genome amplified gDNA was sheared into ~8 kb fragments followed by purification and size-selection using AMPure XP beads (Beckman Coulter). Oxford Nanopore Technology (ONT) sequencing library preparation was then carried out with the Ligation Sequencing Kit (SQK-LSK109) and the library loaded on a MinION Flow Cell and sequenced for 72 hours using a GridION (ONT) controlled by MinKNOW software v20.06.9. Base-calling and demultiplexing were performed within MinKNOW using Guppy v4.0.11. ONT adapters were removed with Porechop v0.2.4 (61). Host reads were filtered out by mapping the Illumina and Nanopore reads against the *Ae. aegypti* reference assembly (Genbank accession: GCF_002204515.2) using Bowtie2 v2.4.2 (62) and Minimap2 v2.23 (63) respectively. Unmapped reads were then assembled using the Unicycler hybrid assembly pipeline (64).

Contigs were visualized and blasted against several *Wolbachia* genomes in Bandage (65) and non-*Wolbachia* sequences were discarded from the assembly.

Comparative genomics

The *w*AlbB-II assembly was compared to three other *w*AlbB isolates for which genome sequences are publicly available – the reference isolate (*w*AlbB-I), which is derived from *Ae. albopictus* mosquitoes caught in Houston, Texas, USA in 1986 and has subsequently been maintained in the *Ae. albopictus* Aa23 cell line (66, 67); an isolate from *Ae. albopictus* caught in St. Augustine, Florida, USA in 2016 (*w*AlbB-FL2016); and an isolate from *Ae. albopictus* caught in Haikou, Hainan, China in 2016 (*w*AlbB-HN2016). *w*AlbB genomes were all reannotated using Prokka v1.14.6 (68) prior to the gene content analysis. Roary v3.13.0 (69) was then used to determine the core and accessory genomes with a 95% identity threshold. The Roary output was manually curated to fix issues with pseudogenes in the accessory genomes by visualizing the genome annotations in the Artemis genome browser v16.0.0 (70). Large indels were confirmed by visual inspection of sequencing depth after mapping the *w*AlbB-II and *w*AlbB-I (SRA accession: SRR7623731) Illumina reads onto the different *w*AlbB genomes with Bowtie2 (Figure S1). Tblastn searches were run to locate WO phage genes, including the homologues of the Octomom and *cif* genes within the genomes using representative sequences. Prophage regions and their eukaryotic modules were then manually re-annotated by following the most recent guidelines (71). Whole-genome and prophage regions synteny were visualized using the R package genoPlotR (72). The maximum likelihood phylogenetic

tree was inferred with RaxML v7.7.6 (73) using a core gene alignment of several Supergroup A and B *Wolbachia* genomes generated by Roary.

The SNP analysis was conducted using the Snippy pipeline v4.6.0 (Seeman, Torsten. Snippy: fast bacterial variant calling from NGS reads; 2020 https://github.com/tseemann/snippy). Illumina reads were mapped onto the different *w*AlbB reference genomes and SNPs were called with minimum mapping quality of 20, 10 reads minimum coverage and 0.9 minimum proportion for variant evidence. From the alignment BAM files, sequencing depth was calculated using Samtools depth v1.13 and visually inspected in R and Artemis to identify large indels and duplicated regions.

Origin of *w*AlbB variants and mosquitoes used in phenotypic assays

The *w*AlbB-I variant used in phenotypic comparisons originates from *Ae. aegypti* mosquitoes that were transinfected in 2005 (24) with the same *w*AlbB infection as the reference isolate found in the Aa23 *Ae. albopictus* cell line. *w*AlbB-I was then transinfected into an *Ae. aegypti* line with an Australian mitochondrial haplotype (33). The *w*AlbB-I genome is almost identical to the *w*AlbB reference genome differing by only four Single Nucleotide Variants (33), suggesting that few genetic changes have occurred since *w*AlbB-I was first transferred to *Ae. aegypti* over 15 years ago (24). In 2015, the *w*AlbB-II variant from the *Ae. albopictus* strain UJU (origin Sulawesi, Indonesia) was transferred into an *Ae. aegypti* line with a Malaysian mitochondrial haplotype through microinjection (6). The donor *Ae. albopictus* UJU embryos carried a triple *Wolbachia* infection,

443 comprising *w*AlbA, *w*Mel and *w*AlbB-II, but incomplete maternal transmission of the triple
444 infection in *Ae. aegypti* allowed for isolation of a single-infection *w*AlbB-II line.

445 wAlbB-I and wAlbB-II populations were backcrossed regularly to natively uninfected
446 populations from Australia and Malaysia respectively to control for genetic background.
447 Uninfected populations were created through antibiotic treatment and the different
448 combinations of nuclear background (Australian or Malaysian), mitochondrial haplotype
449 (Australian or Malaysian) and *Wolbachia* infection status (wAlbB-I, wAlbB-II or uninfected)
450 were generated through reciprocal backcrosses as explained in Ross et al. (2021). Two
451 replicate populations of each combination were created and maintained separately. Both
452 of these were included in *Wolbachia* density and quiescent egg viability measurements,
453 while a single replicate population was tested for *Wolbachia* density under heat stress.

454

455 **_Wolbachia_ detection and density**

456 qPCR assays were used to confirm the presence or absence of *Wolbachia* infection and
457 measure relative density. Genomic DNA was extracted using 250 µL of 5% Chelex 100
458 Resin (Bio-Rad laboratories, Hercules CA) and 3 µL of Proteinase K (20 mg/mL) (Roche
459 Diagnostics Australia Pty. Ltd., Castle Hill New South Wales, Australia). Tubes were
460 incubated for 30 minutes at 65˚C then 10 minutes at 90˚C. *Wolbachia* density was
461 quantified with qPCR via the Roche LightCycler 480. Two primer sets were used to amplify
462 markers specific to mosquitoes (forward primer mRpS6_F [5'-
463 AGTTGAACGTATCGTTTCCCGCTAC-3'] and reverse primer mRpS6_R [5'-
464 GAAGTGACGCAGCTTGTGGTCGTCC-3']), and *w*AlbB (*w*AlbB_F [5'-

CCTTACCTCCTGCACAACAA-3'] and *w*AlbB_R [5'-GGATTGTCCAGTGGCCTTA-3']). For mosquitoes carrying the *w*Mel infection, *Wolbachia* density was determined using w1 primers (w1_F [5'-AAAATCTTTGTGAAGAGGTGATCTGC-3'] and w1_R [5'-GCACTGGGATGACAGGAAAAGG-3'], Lee et al. (2012)). Relative *Wolbachia* densities were determined by subtracting the Cp value of the *Wolbachia*-specific marker from the Cp value of the mosquito-specific marker. Differences in Cp were averaged across 2-3 consistent replicate runs, then transformed by 2^n.

Quiescent egg viability

We measured quiescent egg viability in *Ae. aegypti* populations with different combinations of *w*AlbB infection type (*w*AlbB-I, *w*AlbB-II or uninfected), mitochondrial haplotype (Au or My) and background (Au or My). Six cups filled with larval rearing water and lined with sandpaper strips were placed inside cages of blood fed females from each population. Eggs were collected five days after blood feeding, partially dried, then placed in a sealed chamber with an open container of saturated potassium chloride (KCl) solution to maintain a constant humidity of ~84%. When eggs were 1, 4, 7, 10, 13 and 16 weeks old, small sections of each sandpaper strip were removed and submerged in water with a few grains of yeast to hatch. Four to six replicate batches of eggs were hatched per replicate population at each time point, with 40-125 eggs per batch. Hatch proportions were determined by dividing the number of hatched eggs (with a clearly detached egg cap) by the total number of eggs per female.

Wolbachia density following heat stress

We measured *Wolbachia* density in adults after being exposed to cyclical heat stress during the egg stage. Eggs were collected from *Wolbachia*-infected populations (one replicate population each from *w*AlbB-I Au/Au, *w*AlbB-I Au/My, *w*AlbB-II My/Au, *w*AlbB-II My/My and *w*Mel). Four days after collection, batches of 40-60 eggs were tipped into 0.2 mL PCR tubes (12 replicate tubes per population) and exposed to cyclical temperatures of 29-39°C for 7 d in Biometra TProfessional TRIO 48 thermocyclers (Biometra, Göttingen, Germany) according to Ross et al. (2019). Eggs of the same age from each population were kept at 26°C. Eggs held at 29-39°C and 26°C were hatched synchronously and larvae were reared at a controlled density (100 larvae per tray of 500 mL water). Pupae were sexed and 15 males and 15 females per population and temperature treatment were stored in absolute ethanol within 24 hr of emergence for *Wolbachia* density measurements (see *Wolbachia* detection and density).

Statistical analysis of density and phenotypic traits

Experimental data were analyzed using SPSS Statistics version 24.0 for Windows (SPSS Inc, Chicago, IL). Quiescent egg viability and *Wolbachia* density data were analyzed with general linear (mixed effect) models (GLMs). Replicate populations were pooled for analysis when effects of replicate population exceeded a P-value of 0.1 in prior analyses. Data for each sex were analyzed separately. For *Wolbachia* density, untransformed data (i.e. differences in Cp between *Wolbachia* and mosquito markers, before 2^n transformation) were used for analyses. We ran additional GLMs on *Wolbachia* density in

each nuclear background separately due to significant interactions between background and *w*AlbB variant. For comparisons of *Wolbachia* density at different temperatures, we included temperature treatment (26 or 26-39°C) as a factor. We were unable to perform direct comparisons between *w*Mel and *w*AlbB strains due to using different markers for each strain; we therefore excluded *w*Mel from the overall analysis. We ran separate GLMs for each *w*AlbB variant due to significant two-way interactions. For quiescent egg viability, hatch proportions differed substantially between *w*AlbB-infected and uninfected populations. We therefore ran separate GLMs for *w*AlbB-infected and uninfected populations, with egg storage duration included as an additional factor for this trait. Replicate population (nested within *Wolbachia* infection status) was included as a random factor due to significant effects of replicate population for this trait. Squared egg storage duration was also included as a factor in the GLM due to the non-linear relationship between egg hatch proportion and storage duration in these populations.

Multiplex PCR reaction

DNA was extracted from a pool of five female mosquitoes by crushing tissues in 200 µL of STE buffer. Each sample was then treated with 2 µL of Proteinase K (20 mg/mL) at 65°C for 30 min followed by a 10 min incubation step at 95°C. Tissue debris were removed by centrifugation for 2 min at 1,000 g and the supernatant was diluted 1/5 in water before PCR. Primer pairs specific of each *w*AlbB variant were designed to amplify a target gene present in one variant and absent in the other one. Primers were designed on an AAA-family ATPase protein (DEJ70_04410; forward: 5'-ATGTCTGTTTCTGCGTCTTG-3';

reverse: 5'-ATCGTCTTTATCCAGCCCAG-3'; 303 bp product) for *w*AlbB-I and on the phage tail formation protein I for *w*AlbB-II (WP_015587732.1; forward: 5'-AGAAATACTGCGCTGGGTAA-3'; reverse: 5'-GGATTGCTACATCTAGGCGA-3'; 497 bp product). As a DNA extraction control, primers were also designed to amplify the mosquito 18S gene (forward: 5'-CCCAGCTGCTATTACCTTGA -3'; reverse: 5'-TAAGCAGAAGTCAACCACGA-3'; 752 bp product). The three primer pairs were pooled in a multiplex PCR reaction using the Q5 High-Fidelity DNA Polymerase (New England Biolabs) in a 25 µL final volume as follows: 5 µL of buffer, 0.5 of 10 mM dNTPs, 1.25 µL of each 10 µM primer, 0.25 µL of DNA polymerase, 9.75 µL of water and 2 µL of DNA template. The PCR cycle used was: 98°C for 30s, 35 cycles of 10s denaturation at 98°C – 30s of annealing at 64°C – 1 min extension at 72°C, 2 min final extension at 72°C. PCR product were ran on a 1% agarose gel electrophoresis.

Data availability

The *w*AlbB-II draft genome and raw sequencing data have been deposited at the NCBI GenBank database under the BioProject accession PRJNA800254 (assembly: JAKLOR000000000; Illumina reads: SRR17831854-SRR17832810; Oxford Nanopore reads: SRR17832811).

Acknowledgments

The study was supported by Wellcome Trust (202888, 108508) to SPS and by the National Health and Medical Research Council (1132412, 1118640 [https://www.nhmrc.gov.au]) to

554 AAH. LT and ASF were funded by the MRC (MC_UU_12018/12). The funders had no role
555 in study design, data collection and analysis, decision to publish, or preparation of the
556 manuscript.

557

558 **References**

559 1. Bhatt S, Gething PW, Brady OJ, Messina JP, Farlow AW, Moyes CL, Drake JM,
560 Brownstein JS, Hoen AG, Sankoh O, Myers MF, George DB, Jaenisch T, Wint
561 GRW, Simmons CP, Scott TW, Farrar JJ, Hay SI. 2013. The global distribution
562 and burden of dengue. Nature 496:504–507.

563 2. Ross PA, Callahan AG, Yang Q, Jasper M, Arif MA, Afizah AN, Nazni WA,
564 Hoffmann AA. 2020. An elusive endosymbiont: Does Wolbachia occur naturally in
565 Aedes aegypti? Ecol Evol 10:1581–1591.

566 3. Moreira LA, Iturbe-Ormaetxe I, Jeffery JA, Lu G, Pyke AT, Hedges LM, Rocha
567 BC, Hall-Mendelin S, Day A, Riegler M, Hugo LE, Johnson KN, Kay BH, McGraw
568 EA, van den Hurk AF, Ryan PA, O'Neill SL. 2009. A Wolbachia symbiont in Aedes
569 aegypti limits infection with dengue, Chikungunya, and Plasmodium. Cell
570 139:1268–78.

571 4. Bian G, Xu Y, Lu P, Xie Y, Xi Z. 2010. The Endosymbiotic Bacterium Wolbachia
572 Induces Resistance to Dengue Virus in Aedes aegypti. PLOS Pathog 6:e1000833.

573 5. Walker T, Johnson PH, Moreira LA, Iturbe-Ormaetxe I, Frentiu FD, McMeniman
574 CJ, Leong YS, Dong Y, Axford J, Kriesner P, Lloyd AL, Ritchie SA, O'Neill SL,
575 Hoffmann AA. 2011. The wMel Wolbachia strain blocks dengue and invades

caged Aedes aegypti populations. Nature 476:450–3.

6. Ant TH, Herd CS, Geoghegan V, Hoffmann AA, Sinkins SP. 2018. The Wolbachia strain wAu provides highly efficient virus transmission blocking in Aedes aegypti. PLOS Pathog 14:e1006815.

7. Geoghegan V, Stainton K, Rainey SM, Ant TH, Dowle AA, Larson T, Hester S, Charles PD, Thomas B, Sinkins SP. 2017. Perturbed cholesterol and vesicular trafficking associated with dengue blocking in Wolbachia-infected Aedes aegypti cells. Nat Commun 8.

8. Nazni WA, Hoffmann AA, NoorAfizah A, Cheong YL, Mancini M V, Golding N, Kamarul GMR, Arif MAK, Thohir H, NurSyamimi H, ZatilAqmar MZ, NurRuqqayah M, NorSyazwani A, Faiz A, Irfan F-RRMN, Rubaaini S, Nuradila N, Nizam NMN, Irwan SM, Endersby-Harshman NM, White VL, Ant TH, Herd CS, Hasnor AH, AbuBakar R, Hapsah DM, Khadijah K, Kamilan D, Lee SC, Paid YM, Fadzilah K, Topek O, Gill BS, Lee HL, Sinkins SP. 2019. Establishment of Wolbachia Strain wAlbB in Malaysian Populations of Aedes aegypti for Dengue Control. Curr Biol2019/11/21. 29:4241-4248.e5.

9. Hoffmann AA, Montgomery BL, Popovici J, Iturbe-Ormaetxe I, Johnson PH, Muzzi F, Greenfield M, Durkan M, Leong YS, Dong Y, Cook H, Axford J, Callahan AG, Kenny N, Omodei C, McGraw EA, Ryan PA, Ritchie SA, Turelli M, O'Neill SL. 2011. Successful establishment of Wolbachia in Aedes populations to suppress dengue transmission. Nature 476:454–7.

10. Hoffmann AA, Iturbe-Ormaetxe I, Callahan AG, Phillips BL, Billington K, Axford

598 JK, Montgomery B, Turley AP, O'Neill SL. 2014. Stability of the wMel Wolbachia
599 Infection following Invasion into Aedes aegypti Populations. PLoS Negl Trop Dis
600 8:e3115.

601 11. Tantowijoyo W, Andari B, Arguni E, Budiwati N, Nurhayati I, Fitriana I, Ernesia I,
602 Daniwijaya EW, Supriyati E, Yusdiana DH, Victorius M, Wardana DS, Ardiansyah
603 H, Ahmad RA, Ryan PA, Simmons CP, Hoffmann AA, Rancès E, Turley AP,
604 Johnson P, Utarini A, O'Neill SL. 2020. Stable establishment of wMel Wolbachia
605 in Aedes aegypti populations in Yogyakarta, Indonesia. PLoS Negl Trop Dis
606 14:e0008157.

607 12. Pinto SB, Riback TIS, Sylvestre G, Costa G, Peixoto J, Dias FBS, Tanamas SK,
608 Simmons CP, Dufault SM, Ryan PA, O'Neill SL, Muzzi FC, Kutcher S,
609 Montgomery J, Green BR, Smithyman R, Eppinghaus A, Saraceni V, Durovni B,
610 Anders KL, Moreira LA. 2021. Effectiveness of Wolbachia-infected mosquito
611 deployments in reducing the incidence of dengue and other Aedes-borne
612 diseases in Niterói, Brazil: A quasi-experimental study. PLoS Negl Trop Dis
613 15:e0009556.

614 13. Utarini A, Indriani C, Ahmad RA, Tantowijoyo W, Arguni E, Ansari MR, Supriyati
615 E, Wardana DS, Meitika Y, Ernesia I, Nurhayati I, Prabowo E, Andari B, Green
616 BR, Hodgson L, Cutcher Z, Rancès E, Ryan PA, O'Neill SL, Dufault SM, Tanamas
617 SK, Jewell NP, Anders KL, Simmons CP. 2021. Efficacy of Wolbachia-Infected
618 Mosquito Deployments for the Control of Dengue. N Engl J Med 384:2177–2186.

619 14. Gesto JSM, Ribeiro GS, Rocha MN, Dias FBS, Peixoto J, Carvalho FD, Pereira

620 TN, Moreira LA. 2021. Reduced competence to arboviruses following the
621 sustainable invasion of Wolbachia into native Aedes aegypti from Southeastern
622 Brazil. Sci Rep 11:10039.

623 15. Ulrich JN, Beier JC, Devine GJ, Hugo LE. 2016. Heat Sensitivity of wMel
624 Wolbachia during Aedes aegypti Development. PLoS Negl Trop Dis 10:e0004873.

625 16. Mancini MV, Ant TH, Herd CS, Martinez J, Murdochy SM, Gingell DD, Mararo E,
626 Johnson PCD, Sinkins SP. 2021. High Temperature Cycles Result in Maternal
627 Transmission and Dengue Infection Differences Between Wolbachia Strains in
628 Aedes aegypti . MBio 12:1–13.

629 17. Ross PA, Wiwatanaratanabutr I, Axford JK, White VL, Endersby-Harshman NM,
630 Hoffmann AA. 2017. Wolbachia Infections in Aedes aegypti Differ Markedly in
631 Their Response to Cyclical Heat Stress. PLoS Pathog 13:1–17.

632 18. Ahmad NA, Mancini MV, Ant TH, Martinez J, Kamarul GMR, Nazni WA, Hoffmann
633 AA, Sinkins SP. 2021. Wolbachia strain wAlbB maintains high density and dengue
634 inhibition following introduction into a field population of Aedes aegypti. Philos
635 Trans R Soc Lond B Biol Sci 376:20190809.

636 19. Lau MJ, Ross PA, Hoffmann AA. 2021. Infertility and fecundity loss of wolbachia-
637 infected aedes aegypti hatched from quiescent eggs is expected to alter invasion
638 dynamics. PLoS Negl Trop Dis 15:1–16.

639 20. Hancock PA, Sinkins SP, Godfray HCJ. 2011. Population Dynamic Models of the
640 Spread of Wolbachia. Am Nat 177:323–333.

641 21. Hancock PA, Ritchie SA, Koenraadt CJM, Scott TW, Hoffmann AA, Godfray HCJ.

2019. Predicting the spatial dynamics of Wolbachia infections in Aedes aegypti arbovirus vector populations in heterogeneous landscapes. J Appl Ecol 56:1674–1686.

22. Turelli M, Barton NH. 2017. Deploying dengue-suppressing Wolbachia : Robust models predict slow but effective spatial spread in Aedes aegypti. Theor Popul Biol2017/04/12. 115:45–60.

23. Ruang-areerate T, Kittayapong P. 2006. Wolbachia transinfection in Aedes aegypti: A potential gene driver of dengue vectors. Proc Natl Acad Sci 103:12534–12539.

24. Xi Z, Khoo CCH, Dobson SL. 2005. Wolbachia establishment and invasion in an Aedes aegypti laboratory population. Science (80-) 310:326–328.

25. Mains JW, Kelly PH, Dobson KL, Petrie WD, Dobson SL. 2019. Localized Control of Aedes aegypti (Diptera: Culicidae) in Miami, FL, via Inundative Releases of Wolbachia-Infected Male Mosquitoes. J Med Entomol 56:1296–1303.

26. Bull JJ, Turelli M. 2013. Wolbachia versus dengue: Evolutionary forecasts. Evol Med Public Heal 2013:197–201.

27. Ritchie SA, Townsend M, Paton CJ, Callahan AG, Hoffmann AA. 2015. Application of wMelPop Wolbachia Strain to Crash Local Populations of Aedes aegypti. PLoS Negl Trop Dis 9:e0003930.

28. Martinez J, Klasson L, Welch JJ, Jiggins FM. 2020. Life and death of selfish genes: comparative genomics reveals the dynamic evolution of cytoplasmic incompatibility. Mol Biol Evol https://doi.org/10.1093/molbev/msaa209.

664 29. Lepage DP, Metcalf JA, Bordenstein SR, On J, Perlmutter JI, Shropshire JD,
665 Layton EM, Funkhouser-Jones LJ, Beckmann JF, Bordenstein SR. 2017.
666 Prophage WO genes recapitulate and enhance Wolbachia-induced cytoplasmic
667 incompatibility. Nature 9:243–247.

668 30. Chrostek E, Marialva MSP, Esteves SS, Weinert LA, Martinez J, Jiggins FM,
669 Teixeira L. 2013. Wolbachia Variants Induce Differential Protection to Viruses in
670 Drosophila melanogaster: A Phenotypic and Phylogenomic Analysis. PLoS Genet
671 9:e1003896.

672 31. Chrostek E, Teixeira L. 2015. Mutualism Breakdown by Amplification of
673 Wolbachia Genes. PLOS Biol 13:e1002065.

674 32. Duarte EH, Carvalho A, López-Madrigal S, Costa J, Teixeira L. 2021. Forward
675 genetics in Wolbachia: Regulation of Wolbachia proliferation by the amplification
676 and deletion of an addictive genomic islandPLoS Genetics.

677 33. Ross PA, Gu X, Robinson KL, Yang Q, Cottingham E, Zhang Y, Yeap HL, Xu X,
678 Endersby-Harshman NM, Hoffmann AA. 2021. A w AlbB Wolbachia
679 Transinfection Displays Stable Phenotypic Effects across Divergent Aedes
680 aegypti Mosquito Backgrounds. Appl Environ Microbiol 87:e01264-21.

681 34. Paget MS. 2015. Bacterial Sigma Factors and Anti-Sigma Factors: Structure,
682 Function and Distribution. Biomolecules 5:1245–1265.

683 35. Qayyum MZ, Dey D, Sen R. 2016. Transcription Elongation Factor NusA Is a
684 General Antagonist of Rho-dependent Termination in Escherichia coli. J Biol
685 Chem2016/02/12. 291:8090–8108.

686 36. Bechhofer DH, Deutscher MP. 2019. Bacterial ribonucleases and their roles in
687 RNA metabolism. Crit Rev Biochem Mol Biol 54:242–300.

688 37. Gibbs MR, Fredrick K. 2018. Roles of elusive translational GTPases come to light
689 and inform on the process of ribosome biogenesis in bacteria. Mol
690 Microbiol2017/12/29. 107:445–454.

691 38. Vermassen A, Leroy S, Talon R, Provot C, Popowska M, Desvaux M. 2019. Cell
692 Wall Hydrolases in Bacteria: Insight on the Diversity of Cell Wall Amidases,
693 Glycosidases and Peptidases Toward Peptidoglycan. Front Microbiol.

694 39. Benson TE, Filman DJ, Walsh CT, Hogle JM. 1995. An enzyme-substrate
695 complex involved in bacterial cell wall biosynthesis. Nat Struct Biol 2:644–653.

696 40. Thorup CM, Hanne I, Francis M, Kirsten J, M. WJ, Lone B. 2007. Contribution of
697 Conserved ATP-Dependent Proteases of Campylobacter jejuni to Stress
698 Tolerance and Virulence. Appl Environ Microbiol 73:7803–7813.

699 41. Clausen T, Southan C, Ehrmann M. 2002. The HtrA Family of Proteases:
700 Implications for Protein Composition and Cell Fate. Mol Cell 10:443–455.

701 42. Zhou W, Rousset F, O'Neill S. 1998. Phylogeny and PCR–based classification of
702 Wolbachia strains using wsp gene sequences. Proc R Soc B-Biological Sci
703 265:509–515.

704 43. Armbruster P, Damsky WEJ, Giordano R, Birungi J, Munstermann LE, Conn JE.
705 2003. Infection of New- and Old-World Aedes albopictus (Diptera: Culicidae) by
706 the intracellular parasite Wolbachia: implications for host mitochondrial DNA
707 evolution. J Med Entomol 40:356–360.

708 44. Hu Y, Xi Z, Liu X, Wang J, Guo Y, Ren D, Wu H, Wang X, Chen B, Liu Q. 2020.
709 Identification and molecular characterization of Wolbachia strains in natural
710 populations of Aedes albopictus in China. Parasit Vectors 13:28.

711 45. Richardson MF, Weinert LA, Welch JJ, Linheiro RS, Magwire MM, Jiggins FM,
712 Bergman CM. 2012. Population genomics of the Wolbachia endosymbiont in
713 Drosophila melanogaster. PLoS Genet 8:e1003129.

714 46. Turelli M, Cooper BS, Richardson KM, Chiu JC, Conner WR, Hoffmann AA, Turelli
715 M, Cooper BS, Richardson KM, Ginsberg PS, Peckenpaugh B. 2018. Rapid
716 Global Spread of wRi-like Wolbachia across Multiple Drosophila Report Rapid
717 Global Spread of wRi-like Wolbachia across Multiple Drosophila. Curr Biol
718 28:963–971.

719 47. Wolfe TM, Bruzzese DJ, Klasson L, Corretto E, Lečić S, Stauffer C, Feder JL,
720 Schuler H. 2021. Comparative genome sequencing reveals insights into the
721 dynamics of Wolbachia in native and invasive cherry fruit flies. Mol Ecol 30:6259–
722 6272.

723 48. Goubert C, Minard G, Vieira C, Boulesteix M. 2016. Population genetics of the
724 Asian tiger mosquito Aedes albopictus, an invasive vector of human diseases.
725 Heredity 117:125–134.

726 49. Bordenstein SR, Bordenstein SR. 2011. Temperature affects the tripartite
727 interactions between bacteriophage WO, Wolbachia, and cytoplasmic
728 incompatibility. PLoS One 6.

729 50. Siozios S, Ioannidis P, Klasson L, Andersson SGE, Braig HR, Bourtzis K. 2013.

730 The diversity and evolution of Wolbachia ankyrin repeat domain genes. PLoS One
731 8:e55390.

732 51. Lindsey ARI. 2020. Sensing , Signaling , and Secretion : A Review and Analysis of
733 Systems for Regulating Host Interaction in Wolbachia. Genes (Basel) 11:813.

734 52. Duplouy A, Iturbe-Ormaetxe I, Beatson SA, Szubert JM, Brownlie JC, McMeniman
735 CJ, McGraw EA, Hurst GDD, Charlat S, O'Neill SL, Woolfit M. 2013. Draft
736 genome sequence of the male-killing Wolbachia strain wBol1 reveals recent
737 horizontal gene transfers from diverse sources. BMC Genomics 14.

738 53. du Plessis DJF, Nouwen N, Driessen AJM. 2011. The Sec translocase. Biochim
739 Biophys Acta - Biomembr 1808:851–865.

740 54. Hague MTJ, Shropshire JD, Caldwell CN, Statz JP, Stanek KA, Conner WR,
741 Cooper BS. 2021. Temperature effects on cellular host-microbe interactions
742 explain continent-wide endosymbiont prevalence. Curr Biol 32:1–11.

743 55. Gu X, Ross PA, Rodriguez-Andres J, Robinson KL, Yang Q, Lau M-J, Hoffmann
744 AA. 2022. A wMel Wolbachia variant in Aedes aegypti from field-collected
745 Drosophila melanogaster with increased phenotypic stability under heat stress.
746 bioRxiv 2022.01.02.474744.

747 56. Baião GC, Janice J, Galinou M, Klasson L. 2021. Comparative genomics reveals
748 factors associated with phenotypic expression of Wolbachia . Genome Biol Evol
749 13:1–20.

750 57. Dainty KR, Hawkey J, Judd LM, Pacidônio EC, Duyvestyn JM, Gonçalves DS, Lin
751 SY, O'donnell TB, O'neill SL, Simmons CP, Holt KE, Flores HA. 2021. Wmel

752 wolbachia genome remains stable after 7 years in australian aedes aegypti field
753 populations. Microb Genomics 7:000641.

754 58. Huang B, Yang Q, Hoffmann AA, Ritchie SA, van den Hurk AF, Warrilow D. 2020.
755 Wolbachia Genome Stability and mtDNA Variants in Aedes aegypti Field
756 Populations Eight Years after Release. iScience 23:101572.

757 59. Ross PA, Axford JK, Callahan AG, Richardson KM, Hoffmann AA. 2020.
758 Persistent deleterious effects of a deleterious Wolbachia infection. PLoS Negl
759 Trop Dis 14:e0008204.

760 60. Bolger AM, Lohse M, Usadel B. 2014. Trimmomatic: A flexible trimmer for Illumina
761 sequence data. Bioinformatics 30:2114–2120.

762 61. Wick R. 2017. PorechopGitHub repository. GitHub.

763 62. Langmead B, Salzberg SL. 2012. Fast gapped-read alignment with Bowtie 2. Nat
764 Methods 9:357–9.

765 63. Li H. 2018. Minimap2: pairwise alignment for nucleotide sequences.
766 Bioinformatics 34:3094–3100.

767 64. Wick RR, Judd LM, Gorrie CL, Holt KE. 2017. Unicycler: Resolving bacterial
768 genome assemblies from short and long sequencing reads. PLOS Comput Biol
769 13:e1005595.

770 65. Wick RR, Schultz MB, Zobel J, Holt KE. 2015. Bandage: interactive visualization
771 of de novo genome assemblies. Bioinformatics 31:3350–3352.

772 66. Sinha A, Li Z, Sun L, Carlow CKS, Cordaux R. 2019. Complete Genome

773 Sequence of the Wolbachia wAlbB Endosymbiont of Aedes albopictus. Genome
774 Biol Evol 11:706–720.

775 67. Sinkins SP, Braig HR, O'Neill SL. 1995. Wolbachia superinfections and the
776 expression of cytoplasmic incompatibility. Proc R Soc B Biol Sci 261:325–330.

777 68. Seemann T. 2014. Prokka: rapid prokaryotic genome annotation. Bioinformatics
778 30:2068–2069.

779 69. Page AJ, Cummins CA, Hunt M, Wong VK, Reuter S, Holden MTG, Fookes M,
780 Falush D, Keane JA, Parkhill J. 2015. Roary: rapid large-scale prokaryote pan
781 genome analysis. Bioinformatics 31:3691–3693.

782 70. Carver T, Harris SR, Berriman M, Parkhill J, McQuillan JA. 2012. Artemis: an
783 integrated platform for visualization and analysis of high-throughput sequence-
784 based experimental data. Bioinformatics 28:464—469.

785 71. Bordenstein SR, Bordenstein SR. 2021. The Most Widespread Phage in Animals:
786 Genomics and Taxonomic Classification of Phage WO. bioRxiv
787 2021.11.04.467296.

788 72. Guy L, Roat Kultima J, Andersson SGE. 2010. genoPlotR: comparative gene and
789 genome visualization in R. Bioinformatics 26:2334–2335.

790 73. Stamatakis A. 2014. RAxML version 8: a tool for phylogenetic analysis and post-
791 analysis of large phylogenies. Bioinformatics 30:1312–1313.

792 74. Lee SF, White VL, Weeks AR, Hoffmann AA, Endersby NM. 2012. High-
793 throughput PCR assays to monitor Wolbachia infection in the dengue mosquito

(Aedes aegypti) and Drosophila simulans. Appl Environ Microbiol 78:4740–4743.

75. Ross PA, Ritchie SA, Axford JK, Hoffmann AA. 2019. Loss of cytoplasmic incompatibility in Wolbachia-infected Aedes aegypti under field conditions. PLoS Negl Trop Dis 13:e0007357.

Tables

Table 1. Genome features of sequenced wAlbB genomes

	*w*AlbB-II	*w*AlbB-I	*w*AlbB-FL2016	*w*AlbB-HN2016
Genbank accession	JAKLOR000000000	CP031221.1	CP041923.1	CP041924.1
Geographical origin	Indonesia	Texas	Florida	Hainan
Assembly size (bp)	1,450,135	1,484,007	1,482,279	1,483,853
Contigs (>1000 bp)	16 (9)	1	1	1
GC content (%)	34.3	34.4	34.4	34.4
gene	1,365	1,434	1,426	1,428
CDS	1,324	1,393	1,385	1,387
rRNA	3	3	3	3
tRNA	34	34	34	34
BUSCO complete[a]	328	328	326	328
BUSCO fragment[a]	9	9	11	9
BUSCO missing[a]	95	95	95	95

[a]The BUSCO analysis was run against the alphaproteobacteria_odb10 database.

Table 2. Presence/absence of WO phage core genes in prophage regions. Gene is either present (+) or absent (-). Differences between variants are highlighted in grey. *one copy of the phospholipase D is located outside prophage regions.

Module	Gene annotation (locus tag in *w* AlbB-I)	*w* AlbB-I (Texas, Florida, Hainan)	*w* AlbB-II
Head	Ankyrin repeat protein (DEJ70_04885)	+	+
	Terminase large subunit (DEJ70_04880)	+	+
	Putative terminase small subunit (DEJ70_04890)	+	+
	gpW	-	-
	Portal	-	-
	Minor capsid C	-	-
	Head decoration protein D	-	-
	Major capsid E (DEJ70_06645)	+	+
Connector / baseplate	gpFII (DEJ70_06650)	+	+
	minor tail protein Z	-	-
	Collar	-	-
	gpV	-	-
	PAAR	-	-
	gpW	-	+
	gpJ	-	+
	gpI	-	+
Tail	Tail sheath (DEJ70_05870-DEJ70_05880)	+	+
	Tail tube (DEJ70_05865)	+	+
	gpG/GT (DEJ70_05855 / unannotated downstream ORF)	+	+
	Tape measure (DEJ70_05850)	+	+
	gpU (DEJ70_05845)	+	+
	gpX (DEJ70_05840)	+	+
	Late control D (DEJ70_05835)	+	+
Tail fiber	Baseplate Wedge 3 tail Fiber Network	-	-
	Receptor-binding protein (DEJ70_05895-DEJ70_05900)	+	-
	Tail fiber assembly chaperone (DEJ70_05890)	+	-
	Receptor-binding protein or tail fiber (DEJ70_05885)	+	+
	Tail fiber assembly chaperone	-	-
Recombinase	**Recombinase (DEJ70_04945)**	+	++
Replication and repair	Holliday junction resolvase (DEJ70_04895)	+	+
	AAA family ATPase (DEJ70_04910)	+	+
	AAA family ATPase (DEJ70_04920)	+	+
	RNA_polymerase_sigma_factor (DEJ70_04905)	+	+
	DNA primase (DEJ70_04925)	+	+
Putative lysis	patatin-like phospholipase (DEJ70_06735)	+	+
	phospholipase D (DEJ70_06740, DEJ70_06035)	++*	++*

828 **Table 3. Summary of the SNP analysis.**

	Genome used as reference for SNP calling			
Illumina reads	***w*AlbB-II**	***w*AlbB-I**	***w*AlbB-FL2016**	***w*AlbB-HN2016**
***w*AlbB-II**	**5**	**177**	**793**[a]	**318**[a]
***w*AlbB-MC**	**13**	**195**	**801**[a]	**343**[a]
***w*AlbB-I**	**201**	**0**	**930**[a]	**361**[a]

829 [a]A high proportion of the SNPs against *w*AlbB-FL2016 and -HN2016 show an unusual
830 distribution and may be sequencing errors in the reference genome (Table S2).

831

832

833

834

835

836

837

838

839

840

841

842

843

844

845

846

847

Figures

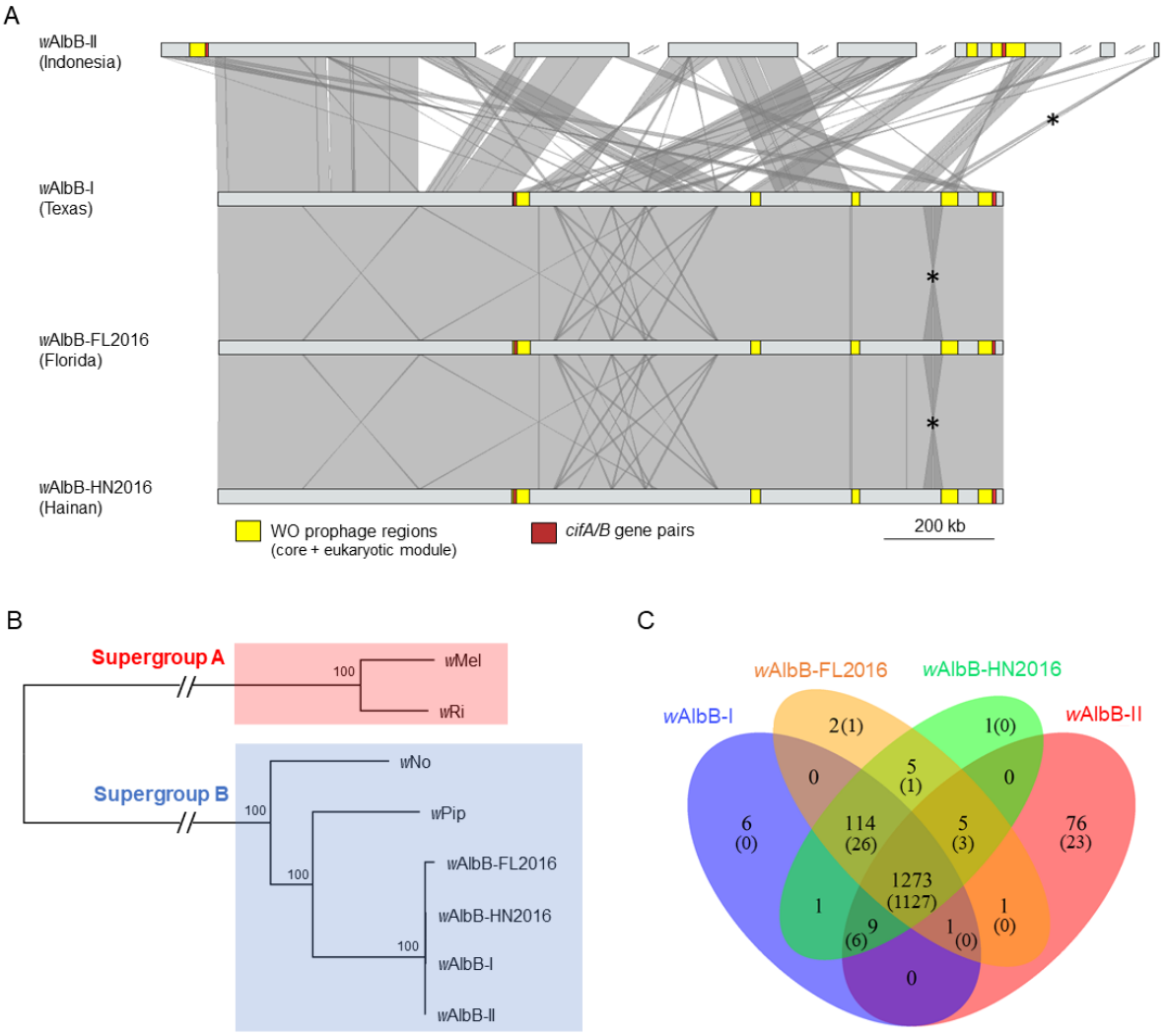

Figure 1. Comparative analysis and phylogeny of *w*AlbB genomes. (A) genome-wide synteny. Grey areas between genomes indicate similarities based on a megablastn comparison. * indicates a seven-gene region that is duplicated in *w*AlbB-I, -FL2016 and -HN2016. Blast hits and contigs < 3,000 bp were excluded from the figure and some contigs were reoriented to improve visualization. (B) Maximum likelihood phylogeny using a concatenated alignment of 614 orthologous genes. Node labels are bootstrap supports calculated from 1,000 replications. (C) Venn diagram showing numbers of orthologs

857 shared between *w*AlbB genomes (numbers in parentheses exclude transposable
858 elements).

859

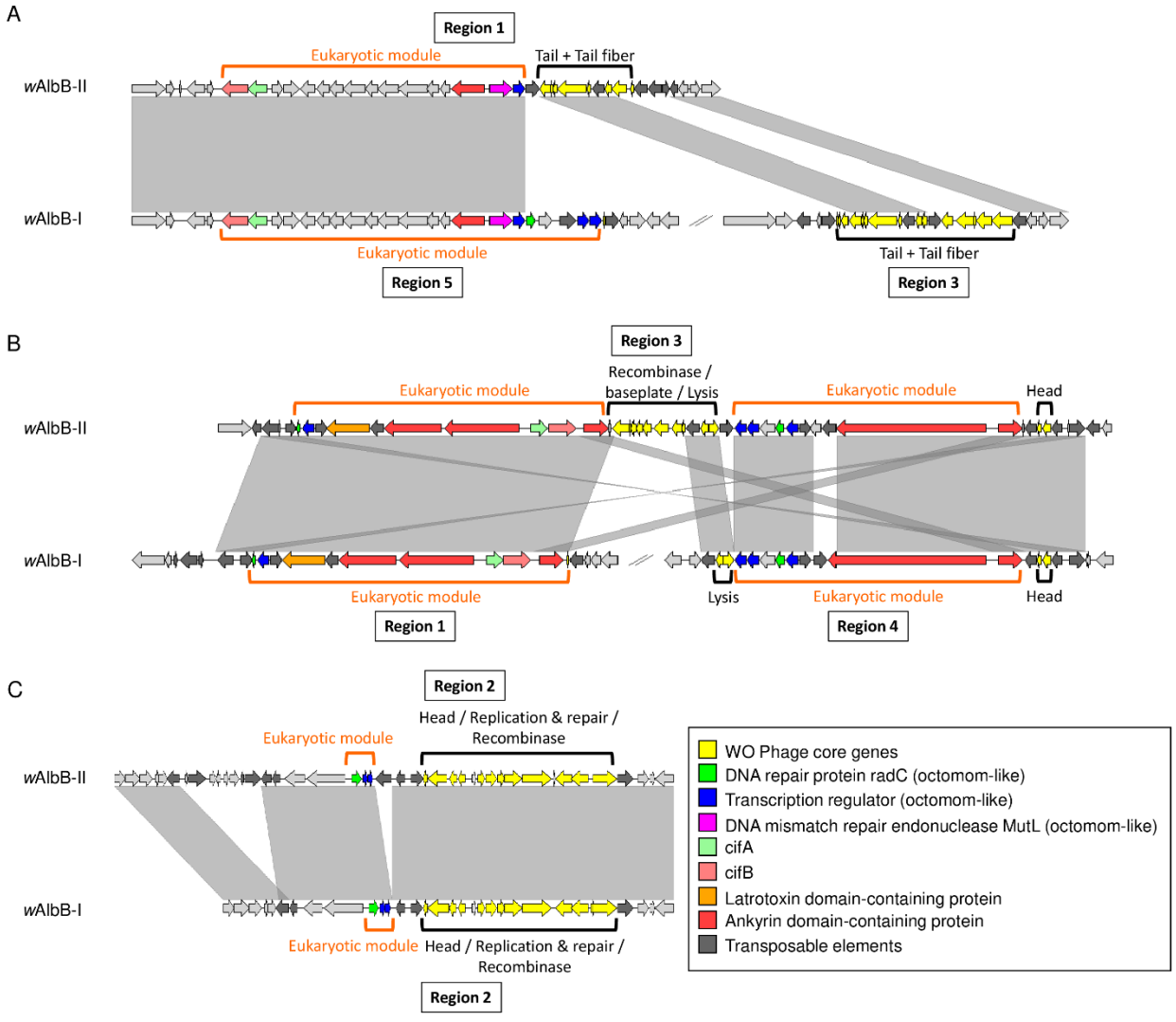

860

861 **Figure 2. Synteny of WO prophage regions between *w*AlbB-I and *w*AlbB-II**
862 **genomes.** Grey areas indicate similarities based on megablastn comparisons. Blast hits
863 < 2,000 bp were excluded from the figure to improve visualization. Panels depict
864 prophage region 1 (A), region 2 (B) and region 3 (C) in the *w*AlbB-II assembly.

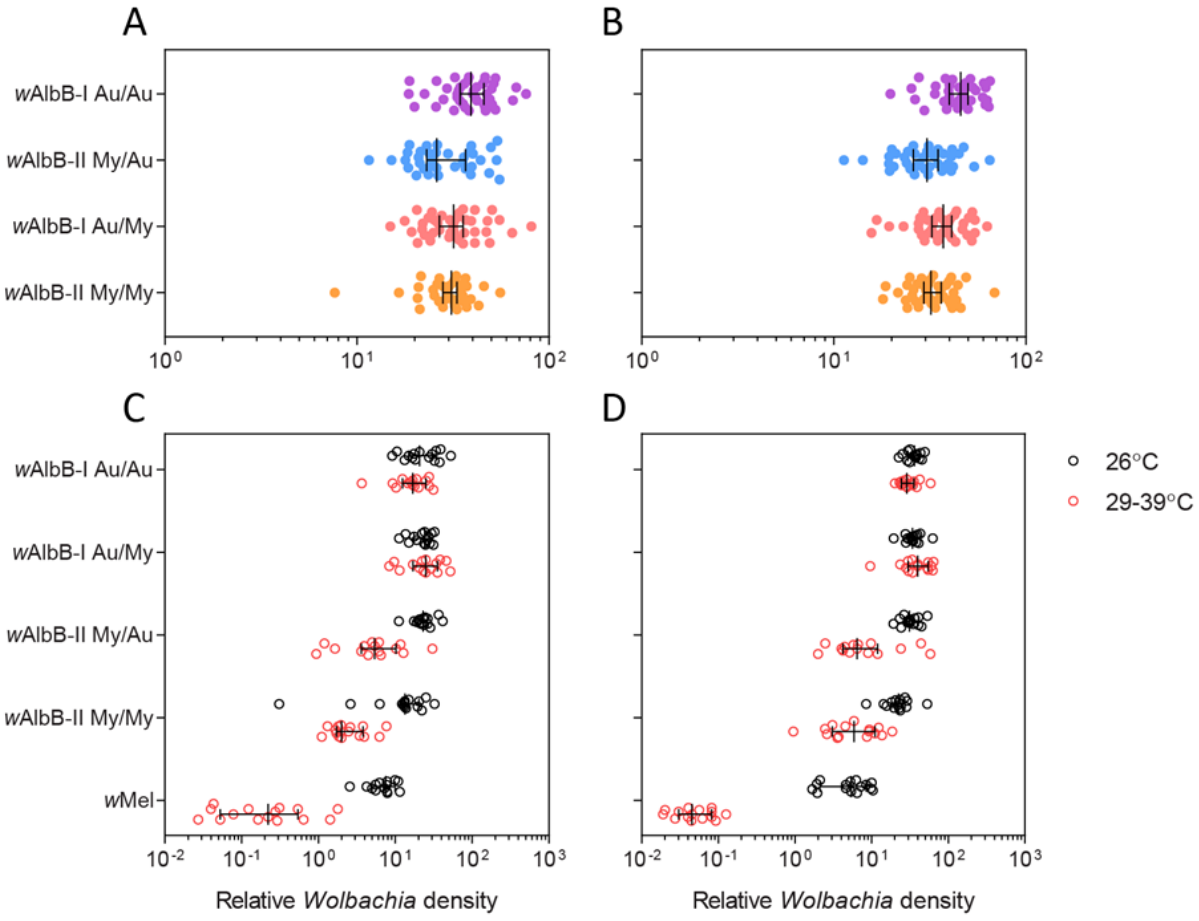

Figure 3. Differences in density between *w*AlbB variants. Female (A) and male (B) *Wolbachia* density in reciprocally-backcrossed *Aedes aegypti* populations. Populations have different combinations of *Wolbachia* infection type/mitochondrial haplotype (*w*AlbB-I and Au or *w*AlbB-II and My) and nuclear background (Au or My). Data from two replicate populations were pooled for visualization. *Wolbachia* density in (C) females and (D) males following exposure to cyclical heat stress during the egg stage. Eggs were exposed to cyclical temperatures of 29-39°C for 7 d (red circles) or held at 26°C (black circles). Each point represents the relative density for an individual averaged across 2-3 technical replicates. Medians and 95% confidence intervals are shown in black lines. Data for *w*AlbB-I and *w*Mel have also been included from (33).

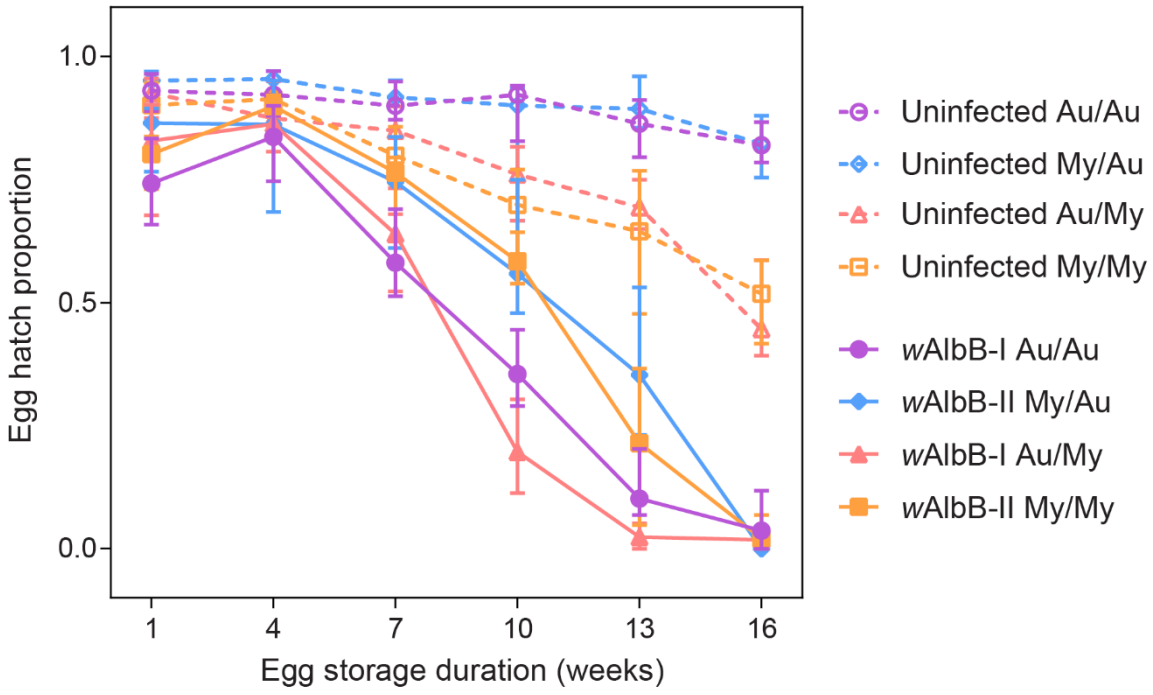

876

877 **Figure 4. Quiescent egg viability of reciprocally-backcrossed *Aedes aegypti***
878 **populations.** Populations have different combinations of *Wolbachia* infection type
879 (*w*AlbB-I, *w*AlbB-II or uninfected), mitochondrial haplotype (Au or My) and nuclear
880 background (Au or My). Data from two replicate populations were pooled for visualization.
881 Symbols show median egg hatch proportions while error bars show 95% confidence
882 intervals. Data for Au/Au and Au/My populations have also been included from (33).

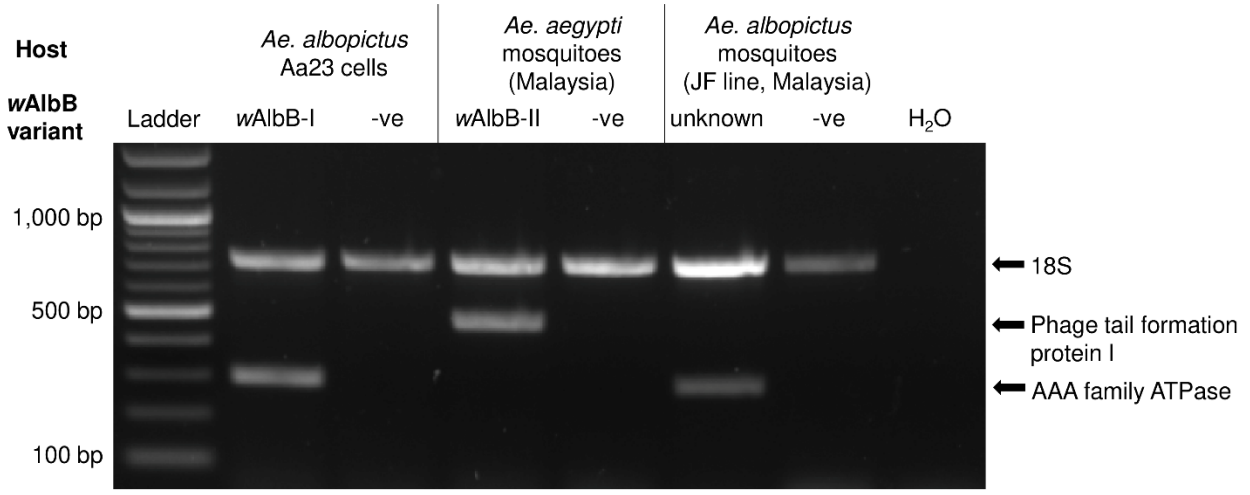

Figure 5. *w*AlbB variant-specific multiplex PCR reaction. DNA was extracted from approximately 1.10^6 cells and five mosquito females for the Aa23 and mosquito samples respectively. -ve: *Wolbachia*-negative controls.

897 **Supplemental Material**

898

899 **Figure S1. Sequencing depth plots.** Mean sequencing depth per 500 bp window of
900 Illumina reads mapped onto (A) *w*AlbB-II, (B) *w*AlbB-I, (C) *w*AlbB-FL2016 and (D)
901 *w*AlbB-HN2016 gemomes.

902

903 **Figure S2. Maximum likelihood phylogenies of horizontally-transferred**
904 **translocase subunit SecA genes.** (A) WP_019236968.1 and (B) WP_019236969.1
905 amino acids were aligned with their homologues and conserved sites (Gblocks) were
906 used to build the phylogenies with PhyML. Node labels are bootstrap supports
907 calculated from 100 replications.

908

909 **Table S1. List of genes being absent in at least one *w*AlbB genome.**

910 **Table S2. List of SNPs between *w*AlbB genomes.**

911 **Table S3. Statistical analysis of differences in density between *w*AlbB variants.**

912 **Table S4. Statistical analysis of *w*AlbB variant densities under heat stress.**

913 **Table S5. Statistical of quiescent egg viability.**

914